# Identification of battery circuit model from EIS data

Brian Ospina Agudelo, Walter Zamboni, Eric Monmasson, Giovanni Spagnuolo

JCGE 2019 Jeunes Chercheurs en Génie Électrique
Oléron – 11-14 juin 2019

# Identification of battery circuit model from EIS data

Brian OSPINA AGUDELO *, Walter ZAMBONI §, Eric MONMASSON ‡ and Giovanni SPAGNUOLO ¶
* ‡ Laboratoire SATIE - Université de Cergy-Pontoise,
SATIE 5 Mail Gay-Lussac – Neuville-sur-Oise 95031 Cergy-Pontoise
* § ¶ DIEM - Università degli studi di Salerno, Via Giovanni Paolo II, 132 - 84084 Fisciano [SA], Italy
* *brian.ospina-agudelo@etu.u-cergy.fr*

**RESUME - La réponse en fréquence d'une batterie peut être utilisée pour évaluer son état de santé. Le renforcement de la fiabilité d'un tel indicateur est l'objet de nombreuses recherches actuelles, notamment dans le domaine des véhicules électriques. Dans ce travail les principales caractéristiques de la réponse en fréquence d'une cellule lithium-ion sont présentées ainsi qu'un circuit équivalent qui est utilisé pour approximer ladite réponse frequentielle. Les équations principales qui régissent l'impédance du circuit équivalent de la batterie sont dans un premier temps établies. Puis, une procédure d'ajustement des paramètres du circuit équivalent sur la base des moindres carrés est proposée et testée sur un jeu de mesures de spectroscopie d'impédance électrochimique. Un tel modèle permettra notamment par la suite la génération de données théoriques de l'impédance d'une batterie et ce, afin de tester des algorithmes originaux d'estimation des paramètres et son état de santé.**

**ABSTRACT - The development of battery health monitoring systems is one of the main research topics related to electrical automotive applications. Some of the most promising approaches in this research area make use of equivalent circuit models, which can be derived from frequency response information of the battery. This work presents the main characteristics of the frequency response of a lithium-ion cell, and an equivalent circuit that can approximate it. The main equations that represent the impedance of the considered equivalent circuit are derived and implemented in Matlab. Theoretical battery impedance data, generated using the aforementioned implementation, can be used for parameters and state estimation algorithms testing. Finally a procedure for the fitting of the parameters in the introduced equivalent circuit is proposed and tested on experimental EIS data.**

**KEYWORDS - Lithium-ion battery frequency response, equivalent circuit based battery impedance model, battery EIS results analysis, battery frequential model parameters fitting.**

## 1. Introduction

The need for reliable energy storage devices has been accentuated in the last years, due to the growing demand for alternative (more clean) methods in the fields of electricity generation, like the ones based on photovoltaic and wind power systems, and transportation, more specifically electric and hybrid electric vehicles. Batteries, particularly lithium-ion technology, are specially well suited for supplying the demands of this applications, due to its compromise between power and energy density and relative long life and environmental friendliness [1].

The performance of the batteries, namely its capability for storing and delivering energy, reduces over time. This degradation takes place due to the charge-discharge cycles and its related temperature and current characteristics [2], but also the battery performance degrade under rest (calendar aging) [3]. This kind of degradation mechanisms normally are manifested as a reduction in the battery capacity or an increase in its equivalent resistance [1].

The characterization of the variations in the performance parameters is important for making corrections to the estimation procedures, failure detection and degradation mechanisms characterization. Normally these variations are quantified making use of figures of merit such as the state of health (SOH), which relates the current value of the performance parameter, normally the capacity or internal resistance, with a reference value (the value obtained in a characterization process performed at a reference moment). It is worth noting that usually the SOH is given as a percentage, with 100 % representing the fresh battery [1].

The methods used for the SOH estimation, mainly on automotive applications, go from the ones based on electro-chemical models of the aging mechanisms, used for the estimation of the performance parameters at a given instant, to the methods that perform the online identification of the parameters on a model of the battery, usually an equivalent

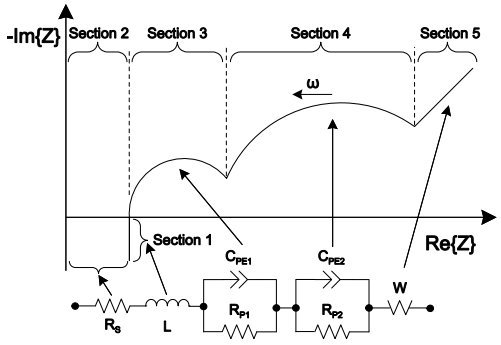


**Figure 1: Qualitative impedance spectrum of a lithium-ion cell and an equivalent circuit with Zarc and Warburg elements that can approximated it.**

circuit-based one, and then establish the SOH making use of previously determined relations [1], [4]. In the later group, one of the most promising approaches is the parameters estimation of equivalent circuit models from battery frequency response data, usually obtained making use of electrochemical impedance spectroscopy (EIS) tests [3], [5]–[7].

This work covers the initial phase of a research project focused on the proposal of an innovative embedded health monitoring unit for batteries developed by using model-based algorithms, ideally oriented to online and on-board applications. This phase is related to the analysis of EIS results and its use for equivalent circuit model parameters fitting, which can be used for SOH estimation purposes. The implementation of an impedance model and a curve fitting procedure of its parameters are presented. The proposed curve fitting procedure is based on the minimization of the distance, in the complex plane, between measured impedance and the model impedance. In this kind of procedures the selection of an adequate initial set of parameters is important, for convergence reasons. A set of initial model parameters is proposed, which improves the convergence of the procedure.

This paper is structured as follows. In section 2, the main characteristics of the typical lithium-ion cell frequency response are presented. An equivalent circuit, that can be used for the approximation of the response, is introduced in section 3. Here the mathematical expressions, obtained for the real and imaginary parts of the circuit impedance, and some results of its implementation in Matlab are also introduced. Finally in section 4, a procedure for the estimation of the parameters of the introduced impedance model is proposed and tested for some EIS experimental data taken from the “Sandia Cell EIS Testing Data” repository [8].

## 2. Battery cell frequency response

The EIS method allows to analyze the impedance of battery cells in a specific range of frequencies. In this way, it is possible to draw conclusions about internal electrochemical processes with different time constants. During an EIS test the goal is to record the amplitudes ratio and the phase difference between the voltage and the current of the battery, which characterize the battery impedance, at multiple frequencies. A general way to do this is to apply a sinusoidal signal, which can be current (galvanostatic) or voltage (potentiostatic), and measuring the response (voltage for the galvanostatic case, and current for the potentiostatic case), repeating the process for all the frequencies of interest.

From the battery impedance magnitude and phase, it is possible to generate Bode plots and, by calculating the impedance real and imaginary parts, a Nyquist plot often called impedance plot. If this is performed for multiple battery operating conditions (temperature, SOC and DC operating point), it is possible to visualize and quantify their influences over the frequency response. For a lithium-ion battery cell, a typical impedance plot is shown in figure 1 [9].

In the qualitative impedance plot shown in figure 1, it is possible to identify five parts which can be associated to particular electrochemical processes [9]. In the first part, an inductive behavior can be seen at high frequencies, related to the inductive reactances of metallic elements in the cell and wires. The presence of an ohmic resistance is revealed by the intersection with the real axis at a non zero value. This corresponds to the sum of the current collectors, active material, electrolyte and separator resistances. The first semi-circle like section is typically associated with the solid electrolyte interface, which tends to be generated during the battery cycling. The fourth part is characterized by a second semi-circle that represents the double layer capacity and charge transfer resistance at the electrodes. Finally, at low frequencies the main effect corresponds to the diffusion processes in the active material of the electrodes, which manifest as a section with a constant slope in the impedance plot.

It is worth noting that measured spectra often show variations with respect at the qualitative curve presented. For example the number of semi-circles can be reduced to one, or the inductive part can exhibit a slope with increments in the real part for increasing frequency. Moreover, the sections referred to as semi-circle like tend to present a depression at its mid-point (not constant radius) [10].

The form of the impedance spectra plot can change significantly with the operating point and the aging of the battery. Low temperatures widen both semi-circles, as consequence of slower chemical processes, and corresponding higher cell impedance. For elevated temperatures both semi-circles tend to merge and can not be distinguished anymore. This means that the time constants of the internal processes associated with the semi-circles get similar. Moreover, it is worth noting that the real axis crossing point increases with the decreasing temperature [9]. The first semi-circle does not show a significant SOC dependency. However, the radius of the second semi-circle increases strongly with the reduction of the SOC (this is especially true for SOC values under 30 %) [9]. The main effect of aging over the frequency response of the battery is the displacement of the plot towards the right, as a manifestation of the increase in series resistance. Some other increments in the radius of the semi-circle like sections are also reported [3], [6], [7].

## 3. Circuit-based impedance models

Circuital models can be used to represent the frequency response of a battery (but normally this kind of circuits can not be directly used for time domain simulations). For a relatively accurate and meaningful reproduction of the impedance spectrum of a battery cell, in the literature equivalent circuits like the one presented in figure 1 are considered [11]. The behavior of the cell at high frequencies is represented by an ideal inductor $L$ and the resistor $R_s$ represents the ohmic resistance of the cell elements. The two semi-circles can be represented using Zarc elements, which correspond to parallel connections between a resistor and a constant phase element (CPE). The impedance of a CPE $Z_{CPE}$ is presented in equation 1, where $Q$ corresponds to a generalized capacitance, $\phi$ to the depression factor, $\omega$ to the angular frequency and $j$ to the imaginary unity [12]. The response at low frequencies is represented by a Warburg element, characterized by a constant phase angle of $45°$ and its impedance can be represented using equation 2, in which $A_w$ corresponds to the diffusion or Warburg coefficient [12].

$$Z_{CPE}(\omega) = \frac{1}{Q\,(j\omega)^{\phi}} \tag{1}$$

$$Z_w(\omega) = \frac{A_w}{\sqrt{\omega}}\,(1-j) \tag{2}$$

CPEs are used instead of capacitors because, when connected in parallel with a resistor forming a Zarc element, the variations in $\phi$ allow to represent the depression often shown in the semi-circles in the impedance plot of a lithium-ion cell. $\phi$ can take values between zero and one, when $\phi = 0$ the Zarc element represents only an ohmic resistance and a value of $\phi = 1$ the response of a RC element is obtained.

The impedance of the circuit presented in figure 1 is defined as:

$$Z_{cw}(\omega) = j\omega L + R_s + \frac{R_{p1}}{1 + R_{p1}Q_1\,(j\omega)^{\phi_1}} + \frac{R_{p2}}{1 + R_{p2}Q_2\,(j\omega)^{\phi_2}} + \frac{A_w}{\sqrt{\omega}} - \frac{A_w}{\sqrt{\omega}}j \tag{3}$$

where $R_{p1}$, $Q_1$ and $\phi_1$ characterize the resistance and CPE parameters of the first Zarc and $R_{p2}$, $Q_2$ and $\phi_2$ do the same for the second Zarc. In order to simplify the implementation of the proposed fitting procedure, the impedance presented in equation 3 can be separated into its real and imaginary parts as follows:

$$\mathrm{Re}(Z_{cw}(\omega)) = R_s + \frac{R_{p1} + R_{p1}^2 Q_1 \omega^{\phi_1} \cos\frac{\phi_1\pi}{2}}{a_1(\omega)} + \frac{R_{p2} + R_{p2}^2 Q_2 \omega^{\phi_2} \cos\frac{\phi_2\pi}{2}}{a_2(\omega)} + \frac{A_w}{\sqrt{\omega}} \tag{4}$$

$$\mathrm{Im}(Z_{cw}(\omega)) = L\omega - \frac{R_{p1}^2 Q_1 \omega^{\phi_1} \sin\frac{\phi_1\pi}{2}}{a_1(\omega)} - \frac{R_{p2}^2 Q_2 \omega^{\phi_2} \sin\frac{\phi_2\pi}{2}}{a_2(\omega)} - \frac{A_w}{\sqrt{\omega}} \tag{5}$$

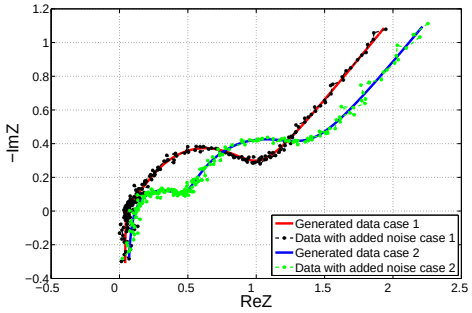


**Figure 2: Impedance plots generated with the implemented model for two different sets of parameters.**

in which $a_1$ and $a_2$ can be obtained by replacing $i$ for 1 or 2 in equation 6 respectively.

$$a_i(\omega) = \left(1 + R_{pi}Q_i\omega^{\phi_i}\cos\frac{\phi_i\pi}{2}\right)^2 + \left(R_{pi}Q_i\omega^{\phi_i}\sin\frac{\phi_i\pi}{2}\right)^2 \tag{6}$$

The equations for the real and imaginary parts of the impedance of the circuit presented in figure 1 were implemented in Matlab using some parameters values within the ranges reported in literature [13], this kind of data generated by simulation may be useful for tests of identification algorithms. The addition of gaussian noise to the data can be considered in order to get a better simulation of experimental data. Figure 2 presents the impedance plots generated using the implemented impedance model in the range of frequencies 10m-10k Hz for two different sets of parameters, introduced in table I, and the curves obtained in both cases after adding Gaussian noise with a signal to noise ratio of 30 dB. The next step in this regard is to add temperature, SOC, electric operating point and aging dependencies to this model, this will allow to generate impedance plots for a given cell under multiple operating conditions.

**Table I: Parameters used for the generation of Nyquist plot with the implemented impedance model**

| Case | $L(\mu H)$ | $R_s(m\Omega)$ | $R_{p1}(m\Omega)$ | $Q_1(S\cdot s^{\phi_1})$ | $\phi_1$ | $R_{p2}(m\Omega)$ | $Q_2(S\cdot s^{\phi_2})$ | $\phi_2$ | $A_w(m\Omega/\sqrt{s})$ |
|---|---|---|---|---|---|---|---|---|---|
| 1 | 5 | 38 | 167.5 | 0.235 | 0.62 | 650 | 0.139 | 0.9 | 270.8 |
| 2 | 5 | 38 | 450 | 0.02 | 0.62 | 650 | 0.4 | 0.9 | 270.8 |

## 4. Circuit parameters estimation procedure

The parameters of the circuit-based impedance model elements can be estimated, making use of a curve fitting procedure of equations 4 and 5 to experimental measurements of impedance data, obtained performing an EIS test for a given set of cell operating conditions. A least squares-based fitting procedure was implemented in order to estimate the values of the parameters of the circuit in figure 1 from experimental impedance results.

The proposed procedure works on data obtained from an EIS test performed for a set of $N$ frequency values:

$$\boldsymbol{\omega} = \begin{bmatrix}\omega_1 & \omega_2 & \cdots & \omega_N\end{bmatrix} \tag{7}$$

The results of the EIS test can be organized in an array such as:

$$\mathbf{Y} = \begin{bmatrix}\boldsymbol{z_1} & \boldsymbol{z_2} & \cdots & \boldsymbol{z_N}\end{bmatrix} = \begin{bmatrix}Re_{z_1} & Re_{z_2} & \cdots & Re_{z_N} \\ Im_{z_1} & Im_{z_2} & \cdots & Im_{z_N}\end{bmatrix} \tag{8}$$

where $z_i$ correspond to the impedance measurement taken at frequency $\omega_i$ with real and imaginary parts $Re_{z_i}$ and $Im_{z_i}$ respectively. Considering the model of the real and imaginary parts of the impedance:

$$\boldsymbol{Z_{CW}}(\omega, \boldsymbol{\theta}) = \begin{bmatrix}Re_{CW}(\omega, \boldsymbol{\theta}) \\ Im_{CW}(\omega, \boldsymbol{\theta})\end{bmatrix} \tag{9}$$

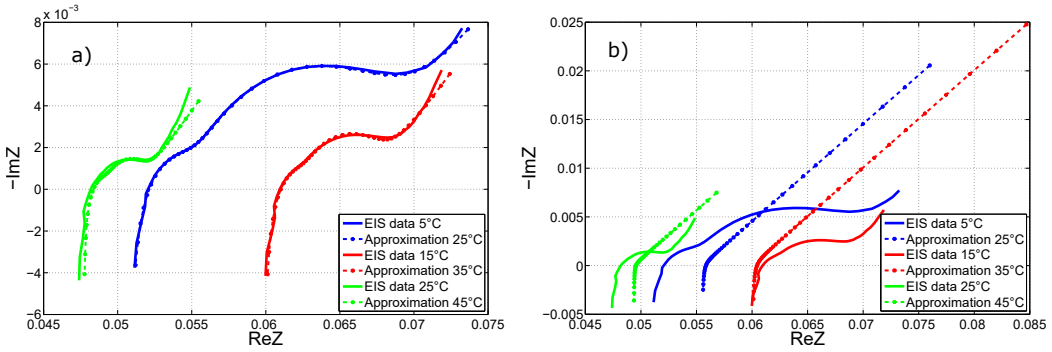


**Figure 3: Results obtained for the proposed fitting procedure using the described experimental EIS data: a) Results obtained using the purposed initial parameters b) Results obtained using zero as initial condition for all the parameters.**

in which $Re_{CW}(\omega, \boldsymbol{\theta})$ and $Im_{CW}(\omega, \boldsymbol{\theta})$ correspond to equations 4 and 5 respectively evaluated for the parameters in vector $\boldsymbol{\theta}$, defined as:

$$\boldsymbol{\theta} = \begin{bmatrix} L & R_s & R_{p1} & Q_1 & \phi_1 & R_{p2} & Q_2 & \phi_2 & A_w \end{bmatrix}^T \tag{10}$$

The problem of finding the parameters of the circuit that allow to approximate the experimental data can be established as the problem of minimizing:

$$\min_{\boldsymbol{\theta}} \sum_{i=1}^{N} \left( [\boldsymbol{z_i} - \boldsymbol{Z_{CW}}(\omega_i, \boldsymbol{\theta})]^T \cdot [\boldsymbol{z_i} - \boldsymbol{Z_{CW}}(\omega_i, \boldsymbol{\theta})] \right) = \min_{\boldsymbol{\theta}} \sum_{i=1}^{N} \left( (Re_{z_i} - Re_{CW}(\omega_i, \boldsymbol{\theta}))^2 + (Im_{z_i} - Im_{CW}(\omega_i, \boldsymbol{\theta}))^2 \right) \tag{11}$$

which basically correspond to minimize the sum of the squares of the euclidean distances between the experimental data and the complex point obtained by evaluating the impedance model at the same frequency. This optimization problem can be solved using a non linear least squares method, such as trust region reflective. The selection of the initial parameters is crucial for the convergence of the solution, in this work the initial parameters values are defined as follows. The initial values for $L$ and $R_s$ are determined from the imaginary and real parts of the impedance measured at the highest frequency value. For $A_w$ an initial approximation is calculated as the mean value of the slope of the plot $Re_{z_i}$ vs $1/\sqrt{w}$ at frequencies under the value for the low frequencies inflection point, which was found analyzing the numerical derivative $dIm_{z_i}/dRe_{z_i}$. The two CPE elements are initially approximated as RC parallel elements by assuming $\phi_1 = \phi_2 = 1$, which allows to approximate initial values of the respective $R_p$ and $Q$ making use of the imaginary part and frequency values at the highest point in the corresponding semi-circle in the impedance plot.

The procedure was tested using EIS results taken from the "Sandia Cell EIS Testing Data" repository [8]. The data corresponds to a $LiCoO_2$ cell LGDBHE21865, with a nominal capacity of 2.5 Ah. The considered impedance measurements were obtained for the cell with a SOC of 0 % using sine signals with an amplitude of 5 $mV$ around to open circuit condition at five different cell temperatures. In this work only the impedance values in the range between 0.1 and 10000 Hz, considering 10 points per decade, were used for the tests performed under 25, 35 and 45$°C$.

The fitting results for the described experimental EIS data are presented in figure 3, for the three temperature values a good approximation of the experimental data was found when the initial parameters were set according to the proposed considerations. In the other hand, when the initial condition was set with all the parameters equal to zero a solution with high errors in the approximation was reached as seen in figure 3. For the three temperatures, the euclidean distance between the experimental and the estimated impedance points was calculated. For all the impedance points in the three cases, the relative values of that differences with respect the experimental impedance amplitudes were under 1.6%, evidencing the goodness of the reached fittings. The main differences between the experimental and approximated data are observed at low frequencies, at which the experimental data presents a curvature that can not be fully represented using the Warburg element.

## 5. Conclusions

The main characteristics of the typical frequency response of a lithium-ion battery, obtained making use of EIS tests, were introduced and some relationships between particular sections in the obtained impedance plot and electrochemical processes were briefly discussed. An equivalent circuit used for the approximation of the impedance of lithium-ion cells, based on CPE and Warburg elements was introduced and the mathematical expressions for the real and imaginary parts of its impedance were derived. These equations can be use to generate impedance data that might be useful during performance tests of parameters estimation algorithms.

A fitting procedure for the parameters on the considered impedance model was presented. This procedure based on the minimization of the sum of the squares of the euclidean distances between experimental and approximated values for the impedance points at the frequencies of interest. Approximations with maximum relative distances to the experimental values under $2\%$ were obtained, when the procedure with the proposed initial conditions was tested using experimental EIS results from the "Sandia Cell EIS Testing Data" repository.

The next efforts in the framework of this research project will be oriented to the introduction of variation of the parameters of the considered model as function of the operating conditions and aging mechanisms in order to develop a tool that allows the generation of impedance data closer to experimental results, which can be used for testing model parameters fitting and states estimation algorithms. Also it is of interest to establish relationships between parameters calculated from frequency response data and battery performance variations, which will allow to design procedures for a battery health monitoring unit oriented to be implemented as part of Battery Management Systems or Battery chargers in automotive applications.

## Acknowledgments

This work is supported by a public grant overseen by the French National Research Agency (ANR) as part of the "Investissements d'Avenir" program (reference: ANR-16-IDEX-0008).

## References

[1] L. Lu, X. Han, J. Li, J. Hua, and M. Ouyang, "A review on the key issues for lithium-ion battery management in electric vehicles," *Journal of Power Sources*, vol. 226, pp. 272–288, 2013. [Online]. Available: http://dx.doi.org/10.1016/j.jpowsour.2012.10.060

[2] A. Eddahech, O. Briat, H. Henry, J. Y. Delétage, E. Woirgard, and J. M. Vinassa, "Ageing monitoring of lithium-ion cell during power cycling tests," *Microelectronics Reliability*, vol. 51, no. 9-11, pp. 1968–1971, 2011. [Online]. Available: http://dx.doi.org/10.1016/j.microrel.2011.07.013

[3] A. Eddahech, O. Briat, E. Woirgard, and J. M. Vinassa, "Remaining useful life prediction of lithium batteries in calendar ageing for automotive applications," *Microelectronics Reliability*, vol. 52, no. 9-10, pp. 2438–2442, 2012. [Online]. Available: http://dx.doi.org/10.1016/j.microrel.2012.06.085

[4] S. M. Rezvanizaniani, Z. Liu, Y. Chen, and J. Lee, "Review and recent advances in battery health monitoring and prognostics technologies for electric vehicle (EV) safety and mobility," *Journal of Power Sources*, vol. 256, pp. 110–124, 2014. [Online]. Available: http://dx.doi.org/10.1016/j.jpowsour.2014.01.085

[5] A. Christensen and A. Adebusuyi, "Using on-board electrochemical impedance spectroscopy in battery management systems," *World Electric Vehicle Journal*, vol. 6, no. 3, pp. 793–799, 2013.

[6] A. Zenati, P. Desprez, H. Razik, A. Zenati, P. Desprez, H. Razik, and L. Ampere, "Estimation of the SOC and the SOH of Li-ion Batteries , by combining Impedance Measurements with the Fuzzy Logic Inference," in *36th Annual Conference on IEEE Industrial Electronics Society IECON 2010*. Glendale, AZ, USA: IEEE, 2010.

[7] H. Wang, L. He, J. Sun, S. Liu, and F. Wu, "Study on correlation with SOH and EIS model of Li-ion battery," *Proceedings of the 6th International Forum on Strategic Technology, IFOST 2011*, vol. 1, no. 12511104, pp. 261–264, 2011.

[8] H. M. Barkholtz, A. Fresquez, B. R. Chalamala, and S. R. Ferreira, "Sandia National Laboratories Battery Cell Testing Data Archive," 2017. [Online]. Available: https://www.sandia.gov/energystoragesafety-ssl/research-development/research-data-repository/

[9] D. Andre, M. Meiler, K. Steiner, H. Walz, T. Soczka-Guth, and D. U. Sauer, "Characterization of high-power lithium-ion batteries by electrochemical impedance spectroscopy. II: Modelling," *Journal of Power Sources*, vol. 196, no. 12, pp. 5349–5356, 2011. [Online]. Available: http://dx.doi.org/10.1016/j.jpowsour.2010.12.102

[10] A. Jossen, "Fundamentals of battery dynamics," *Journal of Power Sources*, vol. 154, no. 2, pp. 530–538, 2006.

[11] D. Andre, M. Meiler, K. Steiner, H. Walz, T. Soczka-Guth, and D. U. Sauer, "Characterization of high-power lithium-ion batteries by electrochemical impedance spectroscopy. II: Modelling," *Journal of Power Sources*, vol. 196, no. 12, pp. 5349–5356, 2011. [Online]. Available: http://dx.doi.org/10.1016/j.jpowsour.2010.07.071

[12] E. Barsoukov and J. R. Macdonald, *Impedance Spectroscopy Theory, Experiment, and Applications*, 2nd ed. Hoboken, New Jersey, USA: Wiley-Interscience, 2005.

[13] B. Wang, S. E. Li, H. Peng, and Z. Liu, "Fractional-order modeling and parameter identification for lithium-ion batteries," *Journal of Power Sources*, vol. 293, no. October, pp. 151–161, 2015. [Online]. Available: http://dx.doi.org/10.1016/j.jpowsour.2015.05.059